HIERARCHICAL COMPUTATION OF PL HARMONIC EMBEDDINGS

T. DUCHAMP, A. CERTAIN, A. DEROSE AND W. STUETZLE

1. Introduction

With the advent of laser scanning systems, extremely large colored meshes are becoming commonplace, and with them the need to efficiently store, transmit, render and edit them. One approach, which has the additional feature of supporting texture mapping is to construct multiresolution representations of meshes. This approach was developed by Lounsbery *et al.* [10, 11], Schröder and Sweldens [13], and Certain *et al.* [2].

Because the method applies only to meshes with *subdivision connectivity*, a algorithm for approximating unstructured meshes by ones with this property was developed by Eck *et al.* [4]. We call this process *remeshing*. The key step in the remeshing algorithm is the construction of "PL harmonic embeddings" from regions of the mesh into the plane. These maps furnish local parameterizations of the mesh which are then used to construct the base complex on which the multiresolution representation lives [4] , as well as to provide efficient texture mapping [2].

In [4] PL harmonic maps were found by the conjugate gradient (CG) algorithm, which, because the problem is a sparse linear least squares problem, has complexity $O(n^2)$ in the number of faces. Constructing PL harmonic maps is, by far, the most time-consuming part of the remeshing process. In this paper, we present a method for computing PL harmonic maps that appears to have complexity $O(n)$, thereby speeding up the remeshing algorithm.

Our approach is to replace the CG algorithm by the preconditioned conjugate gradients (PCG) algorithm [5]. Our preconditioner is a *hierarchical preconditioner*, i.e. it is constructed from a multiresolution decomposition of the space of piecewise linear functions on the domain of the harmonic map, and this multiresolution decomposition is, in turn, crafted from a hierarchy of meshes together with interpolation operators defined in terms of the mean value property of harmonic maps. The inspiration for this approach is previous work of Schröder and Sweldens [12] who used techniques of Dobkin and Kirkpatrick to construct a similar multiresolution expansion for piecewise linear functions.

We recently learned that a similar approach to speeding up the computation of harmonic maps was developed independently by Aaron Lee [9].

Date: July 11, 1997.

This work was partially supported through NSF grants DMS-9402734 and 9661288.

The paper is organized as follows. In Section 2 we discuss the definition of harmonic maps on simplicial surfaces. In Section 3 we define the piecewise linear analogue of harmonic maps. We explain our mesh hierarchy in Section 4, and we use it in Section 5 to construct the multiresolution expansion. Section 6 contains the exposition of our hierarchical preconditioner. We give the results of our numerical experiments in Section 6.2.

2. Harmonic Maps

In this section we show that every simplicial surface has a natural underlying complex-analytic structure. We then use this observation to define the notion of harmonic function on a simplicial surface.

2.1. **Conformal structures.**

Let K be a simplicial complex whose topological realization $M = |K|$ is homeomorphic to a compact 2-dimensional manifold. We call such a complex a *simplicial surface*. Suppose that in addition there is a piecewise linear embedding

$$F : |K| \to \mathbf{R}^3 .$$

We call the pair (K, F) a *(triangular) mesh*.

We will show that the embedding F endows M with a *conformal* (or *complex analytic*) structure. This means that there is a natural notion of complex analytic function on $|K|$; hence, many of the techniques of complex analysis can be used to study $|K|$. In particular, the notion of harmonic function makes sense. As far as we know, the construction presented here was invented by Lipman Bers [1].

There are a number of equivalent definitions of conformal structure. We give here the one that is best suited to our present needs. A conformal structure is given by the following data: a collection of open sets $U_j \subset M$ covering M, together with a collection of homeomorphisms

$$\phi_i : U_i \to \mathbf{C}$$

onto open sets in the complex plane, called a *complex analytic atlas*. The individual maps ϕ_i are called *charts* and they are required to satisfy the compatibility condition that

$$\phi_j \circ \phi_i^{-1} : \phi_i \left(U_i \cup U_j \right) \to \phi_j \left(U_i \cup U_j \right)$$

are all holomorphic (complex analytic). Recall that a complex analytic map is also a conformal map (it preserves angles).; hence, the term "conformal structure". [1]

[1]Surfaces with conformal structure are sometimes called *Riemann surfaces*. The reason for this is that a conformal structure gives enough information to compute the angle between two tangent vectors to a point of M; whereas a Riemannian metric gives an inner product on the space of tangent vectors. Riemannain metrics thus induce conformal structures. Thus a Riemannian metric contains more information than does a conformal structure.

We extend this definition to manifolds with boundary as follows. If M has a boundary ∂M and $\phi : U \to \mathbf{C}$ is a chart whose domain intersects ∂M then the image of ϕ is an open set in the closed upper half plane and ϕ we require ϕ to map points of $\partial M \cap U$ into the real axis.

We now have enough machinery to define the conformal structure on $|K|$ induced by the map f. For each vertex $v \in K$, let $U_v \subset |K|$ denote the interior of the simplicial neighborhood of v, and let $\phi_v : U_v \to \mathbf{C}$ be the chart constructed as follows: If v is an interior vertex of valence n, write U_v as the union

$$U_v = \bigcup_{k=1}^{n} T_k$$

where $T_k = |\{v, v_k, v_{k+1}\}| - |\{v_k, v_{k+1}\}|$, and $v_{n+1} = v_1$ (i.e. T_k is a triangle with the side opposite v removed).

Next let θ_k be the angle of T_k at the vertex v, and set

$$\Theta_1 = 0\,,\ \Theta_k = \sum_{j=1}^{k-1} \theta_j\,, \text{for } k > 1 \text{ and } \Theta = \sum_{j=1}^{n} \theta_j\,.$$

Let $f_k : T_k \to \mathbf{C}$ be the isometry defined by the equations

$$f_k(v) = 0\,, \quad f_k(v_k) = \|v_k - v\| f_k(v_{k+1}) = \|v_{k+1} - v\| e^{i\theta_k}\,,$$

where $\|\ \|$ is the Euclidean norm in $\mathbf{R}^3$. Finally let $\psi : \mathbf{C} \to \mathbf{C}$ be the map $\psi(z) = z^a$ where $a = 2\pi/\Theta$. v to $0 \in \mathbf{C}$. Then The chart ϕ_v is defined as follows:

$$\phi_v(p) = e^{i2\pi/\Theta_k} \psi \circ f_k(p) \text{ for } p \in T_k. \tag{2.1}$$

If v is a boundary vertex of valence $n+1$, write U_v as the union

$$U_v = \bigcup_{k=1}^{n} T_k$$

where $T_k = |\{v, v_k, v_{k+1}\}| - |\{v_k, v_{k+1}\}|$, let $\psi : T \to H = \{z\ :\ Im(z) \geq 0\}$ denote the map, $\psi(z) = z^a$ where $a = \pi/\Theta$, and define ϕ_v by the formula

$$\phi_v(p) = e^{i\pi/\Theta_k} \psi \circ f_k(p) \text{ for } p \in T_k. \tag{2.2}$$

We leave it to the reader to check that the maps $\phi_v : U_v \to \mathbf{C}$ form a complex analytic atlas.

Remark 2.3. *Notice that on the interior of T (but not on its boundary) the map $f_k : T \to \boldsymbol{C}$ is, itself, a conformal coordinated chart. Hence, any computations done on the interior of a face can be done in terms of these coordinates.*

Remark 2.4. *A different atlas for a simplicial surface was given by Grimm and Hugues in* [6]. *Because this atlas is not conformal, it is not suitable for our purposes.*

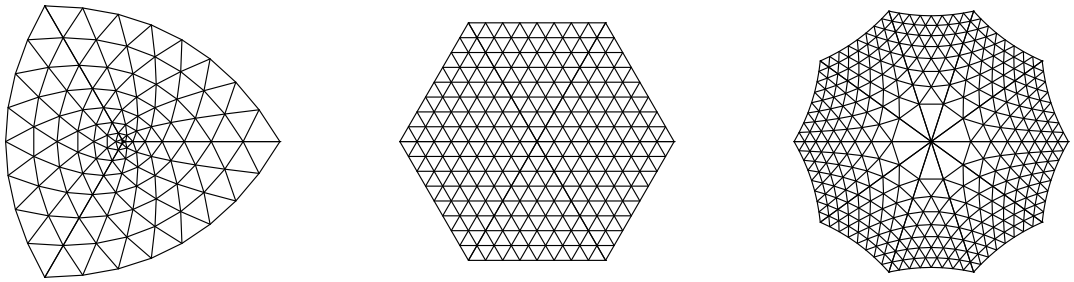

FIGURE 1. Image of simplicial neighborhood of a vertex in the case where all triangles are equilateral. (a) valence = 3, (b) valence = 6, (c) valence = 10.

2.2. **Harmonic maps on Riemann surfaces.** Suppose that M is a compact Riemann surface with piecewise smooth boundary ∂M. Suppose further that M is diffeomorphic to a disk. We want to construct an embedding of M into the plane with prescribed boundary values. More precisely, suppose that

$$F_\partial : \partial M \to \mathbf{R}^2$$

is a piecewise smooth embedding onto the boundary of a compact, convex region $\Omega \subset \mathbf{R}^2$. Our goal is to find a homeomorphism

$$F : M \to \Omega$$

such that $F|_{\partial M} = F_\partial$ which is a diffeomorphism on the interior of M. The construction of f uses the notion of *harmonic map*. The construction is due to Choquet [3] and Kneser [8].

We begin by recalling some basic facts concerning harmonic functions on Riemann surfaces. Let M be a smooth compact surface with boundary ∂M, and let g be a Riemannian metric on M. Suppose $f : M \to \mathbf{R}$ is a smooth function. The *harmonic energy* of f is the quantity

$$E_g[f] = \frac{1}{2}\int_M |df|_g^2 dA_g,$$

where $|\ |_g$ is the norm with respect to g and dA_g is the area element on M induced by g. Let $g = g_{ij}dx^i dx^j$ where x^i, $i = 1, 2$ are local coordinates on M.Then the integrand has the local coordinate expression

$$|df|^2 dA = \sum_{1\le i,j,\le 2} g^{i,j}\frac{\partial f}{\partial x^i}\frac{\partial f}{\partial x^j}\sqrt{\det(g)}\, dx^1 \wedge dx^2.$$

where as usual, g^{ij} denotes the inverse of the matrix g_{ij}, and $\det(g)$ denotes the determinant of g_{ij}.

We now consider the functional

$$E : \mathcal{H} \to \mathbf{R}$$

on the space of smooth functions on M with fixed boundary value $f_\partial : \partial M \to R$, where f_∂ is a smooth function. The critical points for E are called *harmonic functions*, and it is a

classical result that there is a unique harmonic map f assuming the prescribed boundary values f_∂. That map is called the *harmonic extension* of f_∂.

Lemma 2.5. *The harmonic energy depends only on the conformal class of g. That is if $\tilde{g} = e^\lambda g$, for $\lambda : M \to \boldsymbol{R}$ smooth, then*

$$E_g[f] = E_{\tilde{g}}[f]\,.$$

Proof. The lemma follows immediately from the two identities

$$\sqrt{\det(\tilde{g})} = e^\lambda \sqrt{\det(g)} \text{ and } \tilde{g}^{ij} = e^{-\lambda} g^{ij}\,.$$

□

Corollary 2.6. *Let $\phi : (M, g) \to (N, h)$ be a biholomorphism between two compact Riemann surface (possibly with piecewise smooth boundary), and let $f : N \to \boldsymbol{R}$ be a smooth function. Then*

$$E_h[f] = E_g[f \circ \phi]\,.$$

Proof. Let $\tilde{g} = \phi^* h$. Then by the change of variables formula

$$E_h[f] = \frac{1}{2}\int_N |df|_h^2 dA_h = \frac{1}{2}\int_N |d(f\circ\phi)|_{\tilde{g}}^2 dA_{\tilde{g}}$$

But because ϕ is a biholomorphism $\tilde{g}$ is conformally equivalent to g. The result follows from Lemma 2.5. □

As an application of Corollary 2.6, consider the case where M is diffeomorphic to the a disk. The Riemann Mapping theorem states that (M, g) is biholomorphic to the unit disk in the complex plane. We may identify (M, g) with the unit disk in the plane equipped with the Euclidean metric. Letting (u, v) denote the standard coordinates on $\mathbf{R}^2$, we have

$$E_g[f] = \frac{1}{2}\int\int_{u^2+v^2\le 1} \left(\frac{\partial f}{\partial u}\right)^2 + \left(\frac{\partial f}{\partial v}\right)^2 du dv\,.$$

This is the classical "Dirichlet integral." In these coordinates, the Euler-Lagrange equation for E is Laplace's equation

$$\Delta f = \frac{\partial^2 f}{\partial u^2} + \frac{\partial^2 f}{\partial v^2} = 0\,.$$

Planar embeddings of disks. Suppose that M is biholomorphic to a disk and that M has a piecewise smooth boundary ∂M. Let $F_\partial : \partial M \to \mathbf{R}^2$ be a continuous map. The *harmonic extension* of F_∂ is the unique map $F : M \to \mathbf{R}^2$, whose coordinate functions are the harmonic extensions of the coordinate functions of F_∂. Then we have the following theorem (see [3] and [8]).

Theorem 2.7 (Choquet)**.** *Let M be a Riemann surface that is homeomorphic to the disk and $F_\partial : \partial M \to \boldsymbol{R}^2$ be a continuous embedding onto the boundary of a convex region $\Omega \subset \boldsymbol{R}^2$. Let $F : M \to \boldsymbol{R}^2$ be the harmonic extension of F_∂. Then F maps the interior of M diffeomorphically onto Ω.*

Remark 2.8. *If the convexity condition is relaxed, then the extension f exists and is unique, but it is no longer a diffeomorphism, or even a homeomorphism.*

3. PL harmonic functions

In this section, we define the piecewise linear analogue of harmonic functions, called *PL functions* and examine some of their basic properties.

3.1. **Definition of PL harmonic functions.** Consider a mesh $F : |K| \to \mathbf{R}^3$. The underlying space $M = |K|$ has two structures: a PL structure given by the simplicial complex K, and a conformal structure (M, g) induced by the embedding F. The functional E_g depends on the conformal structure, but it can be computed in terms on the PL structure, only.

Let $T_\alpha \subset |K|$, $\alpha = 1, \ldots, n$ be the collection triangular faces of $|K|$. Notice that the union of the interiors of the faces is an open subset of $|K|$ of full measure (i.e. the complement has measure zero). It follows that

$$E_g[f] = \frac{1}{2}\int_M |df|_g^2 dA_g = \frac{1}{2}\sum_\alpha \int_{T_\alpha} |df|_g^2 dA_g\,, \tag{3.1}$$

where $f : M \to \mathbf{R}$ is a piecewise smooth function.

Fix α and let $\phi_v : U_v \to \mathbf{C}$ be the coordinate chart centered at a vertex v of T_α. By virtue of Remark 2.3 and Corollary 2.6, we can compute the integral

$$\frac{1}{2}\sum_\alpha \int_{T_\alpha} |df|_g^2 dA_g\,,$$

by isometrically embedding T into the Euclidean plane and using standard Euclidean coordinates. Let (x, y) be Euclidean coordinates, identify each face T_α with a Euclidean triangle in the (x, y)-plane, and let $f_\alpha : T_\alpha \to \mathbf{R}$ be the restriction of f to T_α. Then

$$\int_{T_\alpha} |df|_g^2 dA_g = \int_{T_\alpha} \left\{ \left| \frac{\partial f_\alpha}{\partial x} \right|^2 + \left| \frac{\partial f_\alpha}{\partial y} \right|^2 \right\} dxdy\,,$$

and consequently

$$E_g[f] = \frac{1}{2}\sum_\alpha \int_{T_\alpha} \left\{ \left| \frac{\partial f_\alpha}{\partial x} \right|^2 + \left| \frac{\partial f_\alpha}{\partial y} \right|^2 \right\} dxdy\,. \tag{3.2}$$

We can evaluate the integral explicitly in the case where f is a piecewise linear function on K. It suffices to evaluate the integral over a single triangle $T = T_\alpha$ on which f is linear. Let v_j, $j = 1, 2, 3$ denote the vertices of T. An elementary computation shows that

$$\frac{1}{2}\int_T \left\{ \left|\frac{\partial f_\alpha}{\partial x}\right|^2 + \left|\frac{\partial f_\alpha}{\partial y}\right|^2 \right\} dxdy = \tag{3.3}$$
$$\frac{1}{2}\left(a^\alpha_{v_1,v_2}|f(v_1)-f(v_2)|^2 + a^\alpha_{v_2,v_3}|f(v_2)-f(v_3)|^2 + a^\alpha_{v_3,v_1}|f(v_3)-f(v_1)|^2\right)$$

where

$$a^\alpha_{v_1,v_2} = \frac{1}{2}\frac{(v_1-v_3)\cdot(v_2-v_3)}{|(v_1-v_3)\times(v_2-v_3)|}$$
$$a^\alpha_{v_2,v_3} = \frac{1}{2}\frac{(v_2-v_1)\cdot(v_3-v_1)}{|(v_2-v_1)\times(v_3-v_1)|}$$
$$a^\alpha_{v_3,v_1} = \frac{1}{2}\frac{(v_1-v_2)\cdot(v_1-v_2)}{|(v_3-v_2)\times(v_1-v_2)|}.$$

The final formula for $E_{harm}[f]$, in the case where f is a piecewise linear function on an complex K, involves certain *spring constants*, which we now define. For $e = \{u, v\}$ an internal edge of K let

$$\kappa_e = a^\alpha_{u,v} + a^\beta_{u,v}\,,$$

where T_α and T_β are the faces of K adjacent to e. If e is a boundary edge let

$$\kappa_{u,v} = a^\alpha_{u,v}\,,$$

where T_α is the face of K adjacent to e. The next theorem summarizes our computation of $E_{harm}[f]$.

Theorem 3.4. *Let $F : K \to \boldsymbol{R}^3$ be a mesh and let (M, g) denote the conformal structure on $M = |K|$ induced by F. If $f : K \to \boldsymbol{R}$ is a piecewise linear function then*

$$E_g[f] = \frac{1}{2}\sum_{\{u,v\}} \kappa_{u,v}\,|f(u)-f(v)|^2\,.$$

By construction, the restriction of E_{harm} to the space of piecewise linear functions with fixed boundary values is a positive definite quadratic functional. Therefore, if

$$f_\partial : \partial\,|K| \to \mathbf{R}$$

is a fixed map, then it has a unique extension to a piecewise linear harmonic function $f : |K| \to \mathbf{R}$ such that $f|_{\partial|K|} = f_\partial$. This extension is called the *piecewise linear harmonic* extension of f_∂.

Note that although the definition of the functional E_g involves integration over faces of K, its *computation* involves only edges of K. Indeed, $E_g[f]$ may be thought of as a "spring energy", where each edge $\{u, v\}$ of K is viewed as a spring with (possibly negative) spring constant $\kappa_{u,v}$.

3.2. **Basic properties of PL harmonic functions.** In this section we discuss some of the basic properties of PL harmonic functions.

Our analysis is based on the quadratic form

$$Q : C^{PL}(K) \times C^{PL}(K) \to \mathbf{R}$$

defined by the equation

$$Q(f,g) = \frac{1}{2} \sum_{\{u,v\} \in K} \kappa_{u,v} \, (f(u) - f(v)) \, (g(u) - g(v)) \, .$$

Notice that

$$E_g[f] = Q(f,f) \, .$$

This observation, combined with the definition of harmonic energy, shows that Q is positive definite inner product on $C^{PL}(K)$.

It is convenient to decompose the space of PL functions on K into functions which vanish on the boundary and those which vanish on the interior. Let $C_0^{PL}(K)$ denote the space of PL functions on K that vanish on ∂K, and let $C_\partial^{PL}(K)$ denote the space of functions that vanish on the interior vertices of K. Then there is a direct sum decomposition

$$C^{PL}(K) = C_0^{PL}(K) \oplus C_\partial^{PL}(K),$$

and we write $f = f_0 + f_\partial$.

Now suppose that $f = f_0 + f_\partial$ is the harmonic extension of f_∂. Our goal is to find f_0. By definition, f_0 is the unique function in $\mathbf{C}_\partial^{PL}(K)$, which minimizes the quantity

$$Q(f,f) = Q(f_0,f_0) + 2Q(f_0,f_\partial) + Q(f_\partial,f_\partial) \, .$$

In particular, for all $h \in C_0^{PL}(K)$, the derivative

$$\frac{d}{dt} E_g[f + t\,h] = \frac{d}{dt} Q(f + th, f + th) = 2Q(f,h) + 2tQ(h,h)$$

vanishes at $t = 0$, and f_0 satisfies the equation

$$Q(f,h) = Q(f_0,h) + Q(f_\partial,h) = 0 \tag{3.5}$$

for all $h \in C_0^{PL}(K)$. Notice that

$$\frac{d^2}{dt^2} Q(f_t,f_t) = 2Q(h,h) > 0$$

for all $h \neq 0$ in $C_0^{PL}(K)$; this shows uniqueness of the harmonic extension.

To solve Equation (3.5) it is convenient to express it in matrix form. For this we need a basis for $C^{PL}(K)$. One obvious choice is the "hat functions". Recall that the *hat function* centered at a vertex $v \in \mathrm{Vert}(K)$, is the piecewise linear function $\hat{\phi}_v$ that assumes the value 1 at v and that is zero at all other vertices. The set of hat functions centered on boundary vertices span $C_\partial^{PL}(K)$ and the set of those centered on interior vertices span $C_0^{PL}(K)$.

Identify the interior vertices of K with the first n integers, and let

$$A_{u,v} = Q\left(\hat{\phi}_u, \hat{\phi}_v\right) \text{ and } b_u = Q\left(\hat{\phi}_u, f_\partial\right) ,$$

for u and v interior vertices of K. Finally let $\mathbf{c} = (c^v)$ be the column vector define by $c^v = f(v)$. Then

$$E_g[f] = \mathbf{c}^t \cdot A \cdot \mathbf{c} + 2\mathbf{c}^t \cdot \mathbf{b} .$$

and Equation (3.5) assumes the form

$$A \cdot \mathbf{c} + \mathbf{b} = 0 . \tag{3.6}$$

It is not difficult to verify that $A_{u,v} \neq 0$, only when u and v are end points of a common edge of K, and because the valence of vertices of most meshes encountered in practice is low, finding the harmonic extension of f_∂ is a sparse linear least squares problem. Methods, such as conjugate gradients, therefore apply. This is the approach taken in [4].

Although finding the PL harmonic extension is a sparse linear least squares problem, it is poorly conditioned (the average valence of a vertex is on the order of 6, and the system (3.6) is highly coupled). The standard conjugate gradients algorithm therefore requires $O(n^2)$ time. We give here a hierarchical algorithm which takes $O(n \log\, n)$ time.

The *PL Laplacian* is the linear operator

$$\Delta_{PL} : C^{PL}(K) \to C^{PL}(K)$$

on the space of piecewise linear functions on K defined by the formula

$$\Delta_{PL} f(u) = \sum_{\{u,v\} \in K} \kappa_{u,v} \left(f(v) - f(u)\right) . \tag{3.7}$$

In terms of the PL Laplacian

$$\begin{aligned} Q(f,g) &= \frac{1}{2} \sum_{\{u,v\} \in K} \kappa_{u,v} \, \left(f(u) - f(v)\right) \left(g(u) - g(v)\right) \\ &= -\frac{1}{2} \sum_{u \in \mathrm{Vert}(K)} g(u) \, \Delta_{PL} f(u) = -\frac{1}{2} \sum_{u \in \mathrm{Vert}(K)} f(u) \, \Delta_{PL} g(u) . \end{aligned}$$

The next proposition is an immediate consequence of our analysis thus far.

Theorem 3.8. *A function $f \in C^{PL}(K)$ is the PL harmonic extension of f_∂ if and only if*

$$\Delta_{PL} f(v) = 0$$

for every interior vertex v of K and agrees with f_∂ on ∂K.

From the definition of the PL Laplacian the condition $\Delta_{PL} f(v) = 0$ is equivalent to the important *mean-value property* that

$$f(v) = \frac{\sum_{j=1}^{d} \kappa_{v,v_j} f(v_j)}{\sum_{j=1}^{d} \kappa_{v,v_j}} . \tag{3.9}$$

where $v_1, \ldots, v_d$ are the vertices of K adjacent to v.

The mean-value property of PL harmonic functions plays a crucial role in our analysis. The property that the value of a PL harmonic function at a vertex is a weighted average of its values at neighboring vertices forms the basis of the interpolation scheme that we present in Section 5.

We exploit the mean-value property in Section 4 where we construct a vertex hierarchy in which vertices located at a given level are isolated from one another by vertices at a coarser level. The mean-value property of PL harmonic functions can then be used to craft interpolation operators that extend PL functions at coarse levels to increasingly fine levels (see Section 5. This interpolation process, in turn forms the basis of our "hierarchical preconditioner".

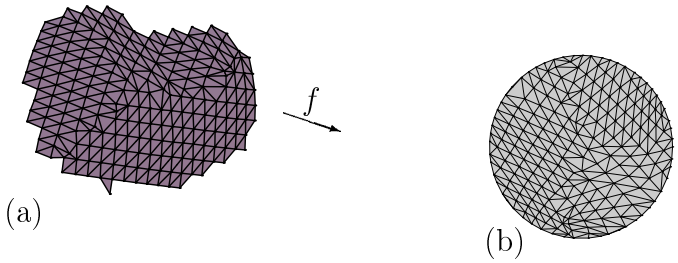

FIGURE 2. (a) A mesh (K, F), with $|K|$ homeomorphic to a disk. (b) A PL harmonic embedding that maps ∂K into the unit circle.

3.3. **PL harmonic maps.** Our analysis of PL harmonic functions extends to maps. We call a piecewise linear map $F : |K| \to \mathbf{R}^2$ a *PL harmonic map* if each of its component functions is PL harmonic. It is an immediate consequence of our analysis of PL harmonic functions that K is homeomorphic to a disk, then every PL harmonic map F is uniquely determined by its boundary values; we call it the PL harmonic extension of the boundary map. Figure 2 shows a harmonic map in the case where the boundary values all lie on the boundary of a unit circle in the plane.

It is important to note that Theorem 2.7 does not hold for PL harmonic maps. *There is no guarantee that PL harmonic maps are embeddings.* Figure 3 gives an example where the image of the boundary is convex, yet the PL harmonic extension fails to be an embedding. Because the PL maps are dense in the Sobolev space of functions with square integrable first derivative, Theorem 2.7 guarantees that after repeated subdivision, the PL harmonic extension will approach an embedding in the L^2-sense. We conjecture that if all spring constants are positive then every PL harmonic map with convex boundary values is an embedding, but we have not yet shown this.

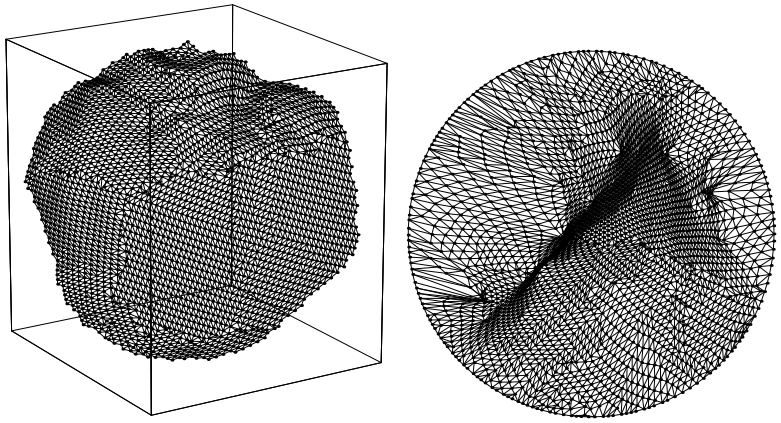

FIGURE 3. A PL harmonic map from a complex K with convex boundary values, yet is not an embedding.

4. Hierarchical reduction of unstructured meshes

A key component of our algorithm is a mesh reduction algorithm. It is based on ideas of Kirkpatrick [7] and Schroeder-Zarge-Lorensen [14]. KIrkpatrick considered only planar meshes, but his method easily generalizes to arbitrary simplicial surfaces.

The goal of the algorithm is to construct a hierarchy of increasingly coarse, simplicial surfaces

$$K_0 = K,\, K_{-1},\, , K_{-2},\, \ldots\, , K_{-J}\,,$$

with nested vertex sets and whose underlying topology agrees with that of K(see Figure 4). For $k = 0, 1, 2, \ldots$, we call the complex K_{-k}, the *reduced complex at depth* $-k$. Such a hierarchy of surfaces defines a hierarchy of meshes

$$F_{-k} : |K_{-k}| \to \mathbf{R}^3$$

defined by $F_{-k}(v) = F(v)$ for all $v \in \mathrm{Vert}(K_{-k})$. We view F_{-k} as an approximation of the original mesh F. Thus, we also require that the reduction algorithm roughly respect the geometry defined by F. Although the spaces $|K_k|$ are all homeomorphic, we do not require the PL maps F_k to be embeddings.

Roughly speaking, the reduction algorithm proceeds by selecting an independent set[2] S of vertices of K that have valence strictly less than 12. Each vertex of S is surrounded by a polygonal neighborhood. Retriangulating the polygonal neighborhoods of the vertices of S after first removing the central vertex results in a new simplicial complex, with fewer vertices. Iterating this process yields the hierarchy. For meshes that are homeomorphic to disks, the set S is guaranteed to contain at least $1/24$ of the total number of vertices [7], but typically it contains $1/4$. Thus the number of iterations required to completely reduce the mesh is

[2]A set is said to be *independent* if no two vertices are joined by an edge of K.

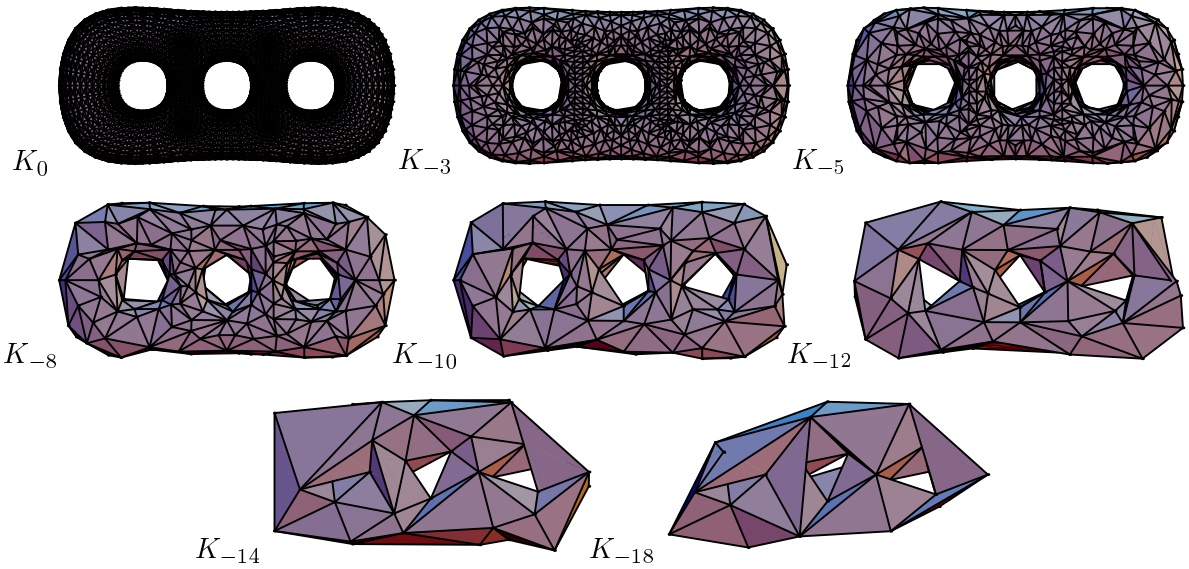

FIGURE 4. Results of the reduction algorithm applied to the mesh K_0 (11776 faces). The algorithm terminates with $K_{-J} = K_{-18}$ (60 faces).

on the order of $\log n$ in the number of vertices. Figure 4 illustrates the result of our mesh reduction algorithm applied to a topologically complex mesh.

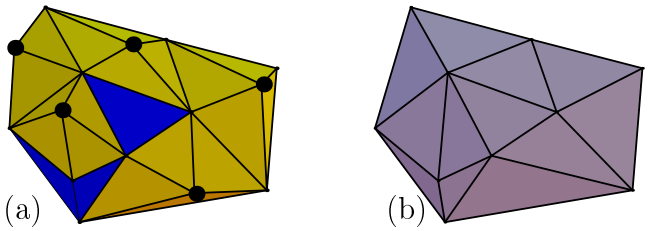

FIGURE 5. (a) An independent set S of vertices in K (shown as heavy dots), together with polygonal neighborhoods of each vertex of S (lightly shaded regions). (b) The result K_{-1} obtained by retriangulating the polygonal neighborhoods of vertices of S.

Our criterion for adding a vertex v to S is that it have valence less than 12 and that we can retrangulate the polygonal neighborhood surrounding it without changing the underlying topology. A secondary consideration is that the radius of the neighborhood be relatively small. This leads to the following definitions.

Definition 4.1. *If $v \in K$ is a vertex, let $P_v \subset |K|$ be the polygonal neighborhood of all faces of K containing v. The* radius, *r_v of P_v is the length of the longest edge of K joining v to a vertex in the boundary of P_v. P_v is said to be* non-degenerate *if no two non-adjacent boundary vertices in P_v (excluding v in the case where v is a boundary vertex of K) are connected by an edge of K. Let $\{v, v_1, \ldots, v_m\}$ be the vertex set of P_v. A* retriangulation *of P_v is simplicial complex P'_v whose vertex set is $\{v_1, \ldots, v_m\}$ and that is homeomorphic to a P_v.*

The following lemma (whose proof we leave to the reader) highlights the importance of this notion of non-degenerate polygon.

Lemma 4.2. *Let P_{v_0} be a non-degenerate polygonal neighborhood of a vertex v of a simplicial surface K, and let K' be the simplicial complex obtained by replacing P_v by a retriangulation P'_v. Then the underlying spaces $|K|$ and $|K'|$ are homeomorphic.*

Remark 4.3. *The non-degeneracy criterion in Lemma 4.2 is a conservative one. A necessary and sufficient condition for $|K|$ and $|K'|$ to be homeomorphic is that*

$$Edges(K) \cap Edges(P'v) = \{\{v_n, v_1\}, \{v_1, \mathbf{v}_2\}, \ldots \{v_{n-1}, v_n\}\}$$

if v in an interior vertex and that

$$Edges(K) \cap Edges(P'v) = \{\{v_1, \mathbf{v}_2\}, \ldots \{v_{n-1}, v_n\}\}$$

is v is a boundary vertex. We choose that more conservative criterion because it is faster to test and gives satisfactory results.

Reduction step. With these definitions we can present a formal description of our reduction step.

1. Initially let $K_{-1} = K$, $S = \emptyset$, and let V denote the set of all vertices of K of degree at most 11, sorted according to the radius of the polygonal neighborhood of each vertex.
2. Let v be the first element of V centered at a non-degenerate polygon of K_{-1}. If there are no such vertices exit; otherwise add v to S.
3. Remove all vertices of P_v from V.
4. Let K'_{-1} denote the complex obtained by retriangulating P_v. In our implementation, this is accomplished by performing an edge collapse along a shortest length, radial edge of P_v (see Figure 5).
5. Set $K_{-1} = K'_{-1}$ and go to Step (2).

Let S_0 denote the set of vertices of K not in K_{-1}. Observe that S_0 is a non-degenerate set and that K_{-1} is the simplicial complex obtained from K by retriangulating the polygon neighborhood of each vertex of S_0. Iterating the reduction step yields the sequence K_{-k}, $k = 0, \ldots, J$ (see Figure 4) together with a sequence of vertex sets S_{-k} (we set S_j equal to the full vertex set of K_{-J}). Notice also that every vertex of K is contained in precisely one of the sets S_{-k}. We say that a vertex $v \in S_{-k}$ is a *depth k* vertex. Figure 6 contains a description of our mesh reduction algorithm in pseudocode.

```
k ← 0;
K_0 ← K;
V ← {v ∈ Vert(K_{-k}) : valence(v) < 12 and P_v non-degenerate };
sort V by radius of polygonal nbhd;
repeat{
    k ← k + 1; K_{-k} ← K_{-(k-1)}; S_{-k} = ∅;
    while ( V ≠ ∅) do {
        v ← First(V) such that P_v is non-degenerate ;
        if( v == NULL) break;
        S_{-k} ← S_{-k} ∪ {v};
        V ← (V − Vert(P_v));
        K_{-k} ← (collapse shortest radial edge of P_v);
        }
    V ← {v ∈ Vert(K_{-k}) : valence(v) < 12 and P_v non-degenerate };
    sort V by radius of polygonal nbhd;
}until (V == ∅)
```

FIGURE 6. Pseudocode description of the mesh reduction reduction algorithm.

5. A hierarchical basis for $C^{PL}(K)$.

In this section we show how the hierarchy of meshes $\{K_{-k}\}$ described in the previous section leads to a multiresolution decomposition

$$C^{PL}_{-J} \hookrightarrow C^{PL}_{-(J-1)} \hookrightarrow \cdots \hookrightarrow C^{PL}_{-1} \hookrightarrow C^{PL}_0 = C^{PL}(K)$$

of the space $C^{PL}(K)$ of piecewise linear functions on K. The inclusions are *interpolation operators*

$$\iota_k : C^{PL}(K_{-(k+1)}) \to C^{PL}(K_{-k})$$

for $k = 0, 1, \ldots, J-1$.

These interpolation operators are constructed from the mean-value property of PL harmonic functions. We use the geometry of the mesh $F_k : K_{-k} \to \mathbf{R}^3$ to compute spring constants and construct our interpolation operators to mirror the mean-value property. If f is a PL function on $K_{-(k+1)}$, to extend it to K_{-k} we need only specify its values on S_{-k}, and we do this via the mean-value property.

Here is the formal definition of ι_k. Choose a PL map $f \in C^{PL}(K_{-(k+1)})$, and let $f' = \iota_k(f)$. Because ι is interpolating, set

$$f'(v) = f(v) \text{ for } v \text{ a vertex of } K_{-(k+1)}.$$

For $v \in S_k \cup \partial K_{-k}$, we set $f'(v) = 0$ and for $v\ in S_k - \partial K_{-k}$ we set

$$f'(v) = \sum_{j=1}^{n} w_{v,j}\, f(v_j)\,.$$

where n_v is the degree of v in the complex K_{-k}, v_1, ... ,v_{n_v} are the vertices of K_k incident to v, and

$$w_{v,j} = \frac{\kappa_j}{\sum_{i=1}^{n_v} \kappa_i}$$

with κ_j the spring constant associated to the edge $\{v, v_j\}$ in K_{-k}. Next choose a vertex $v \in S_{-k}$ and let $\hat{\phi} \in C^{PL}(K_{-k})$ be the "hat-function" centered at v.

To obtain a multiresolution decomposition of function in $\mathbf{C}^{PL}(K)$, repeatedly apply the interpolation to obtain function

$$\psi_v^{-k} = \iota_0 \circ \iota_1 \circ \ldots \iota_{k-1}(\hat{\phi}_v^{-k})\,.$$

Because they share many properties with the lazy piecewise linear wavelets formed from hat functions (see [15]) we call these functions *lazy PL harmonic wavelets*. It is not difficult to show that

$$C^{PL}(K) = \bigoplus_{k=-J}^{0} W^{(-k)}(K)$$

where

$$W^{(-k)}(K) = \text{span}\{\psi_v^{-k} \ : \ v \in S_k\}$$

are the level $-k$ lazy PL harmonic wavelets. Although, this decomposition is not orthogonal in the L^2-sense. Figure 7 shows the lazy PL harmonic wavelets as a graphs over the harmonic embedding of a disk onto a region in the plane. The z-coordinate is the value of the basis function.

5.1. **Analysis and Synthesis.** As with ordinary wavelets, we can quickly convert between the hat function and PL harmonic wavelet expansions of a function $f \in C^{PL}(K)$.

Let $\hat{\phi}_v$, $v \in \text{Vert}(K)$, denote the hat function centered at v. Then any function $f \in C^{PL}(K)$ has a expansion

$$f = \sum_{v \in \text{Vert}(K)} c^v\, \hat{\phi}_v \tag{5.1}$$

where $c^v = f(v)$, as well as an expansion of the form

$$f = \sum_{k} \sum_{v \in S_{-k}} d^v\, \psi_v^{-k}\,. \tag{5.2}$$

(We do not need a subscript on d^v because each vertex appears at only one depth.)

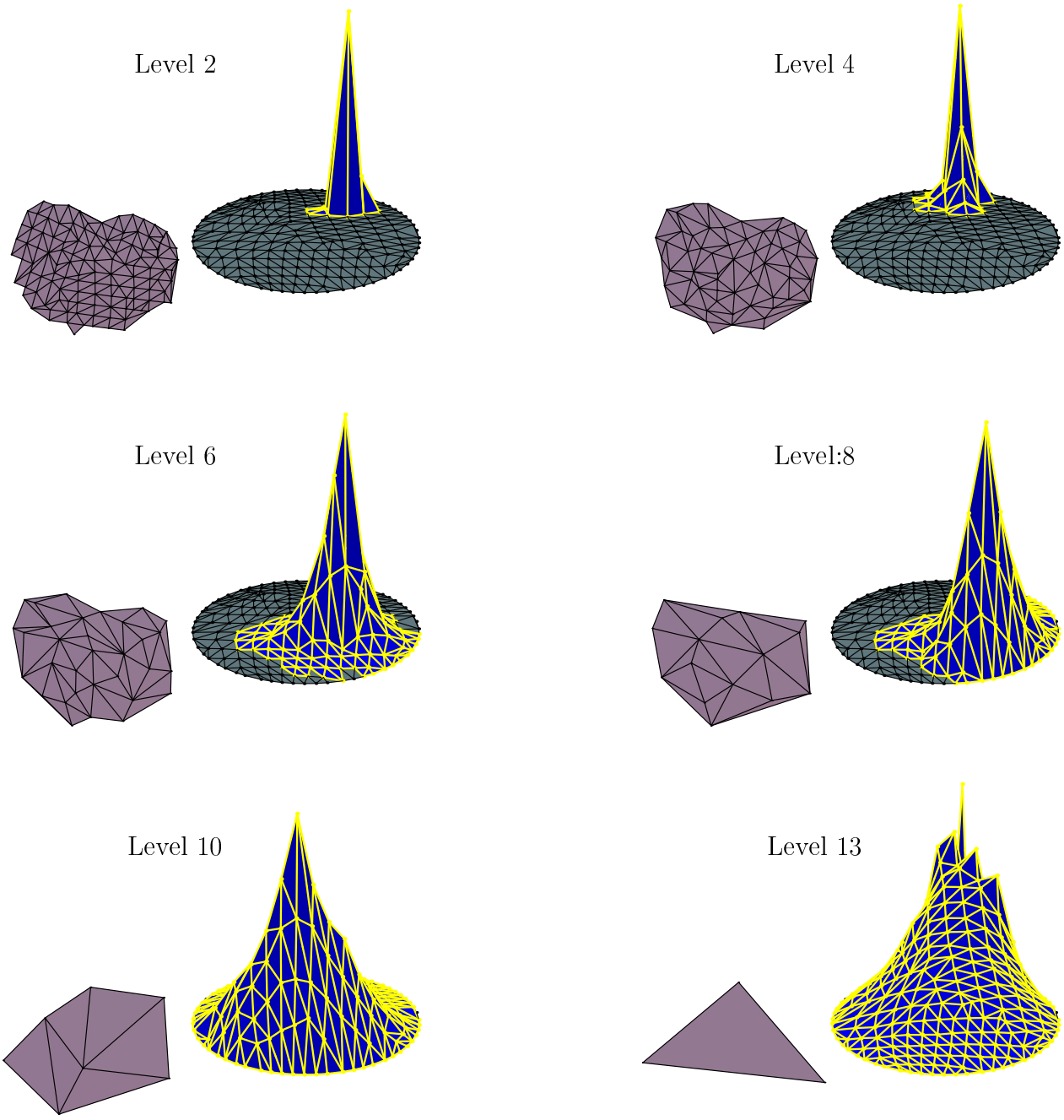

FIGURE 7. "Lazy PL harmonic wavelets" associated to the mesh hierarchy obtained by applying the reduction algorithm applied to the disk in Figure 2. The coarsest depth wavelet (bottom, right) is centered on boundary vertices, causing its irregular shape.

Analysis is the (linear) operation of computing the coefficients d^v from c^v, and *synthesis* is the (linear) operation of computing c^v from d^v. Both analysis and synthesis can be performed rapidly and efficiently by means of the pseudo-code in Figure 8. Notice that if c is not needed later, the computation of d from c can be done "in place", as can the computation of c from d.

Analysis algorithm.

for all $v \in \mathsf{Vert}(K)$ do $d^v \leftarrow c^v$;
for $(k = 0; k < J; k{+}{+})$ do
  for all $v \in S_{-k}$ such that $\mathbf{v} \notin \partial K$ do

$$d^v \leftarrow d^v - \sum_{i=1}^{n_v} w_{v,i}\, d^{v_i}$$

Synthesis algorithm.

`for` all $v \in \mathsf{Vert}(K)$ do $c^v \leftarrow d^v$;
for $(k = J - 1; k \geq 0; k{-})$ do
  for all $v \in S_{-k}$ such that $\mathbf{v} \notin \partial K$ do

$$c^v \leftarrow c^v + \sum_{i=1}^{n_v} w_{v,i}\, c^{v_i}$$

FIGURE 8. The analysis and synthesis algorithms. (n_v denotes the degree of $v \in S_{-k}$ in K_{-k}; v_i are the vertices adjacent to v; and κ_i is the spring constant associated to the edge $\{v, v_i\}$ in K_{-k}. Notice that because $n_v < 12$, both the analysis and synthesis algorithms have $O(n)$ order of growth in the number of vertices of K.)

---

6. Preconditioned conjugate gradients

The hierarchical basis that we constructed in the previous section can be used to construct a "preconditioner" for the system, permitting us to use the *preconditioned conjugate gradients* (PCG) algorithm[5, Page 527].

Recall (see [5]) that CG is an iterative steepest descent algorithm for finding local minima of a function. The performance of CG is heavily dependent on the basis used to compute the gradient of the objective function. The natural basis to use is the basis of hat functions of the mesh (this basis is the one in which the harmonic energy $E[f]$ can be most easily computed). On the other hand, the hierarchical basis of PL harmonic wavelets consists of functions that are roughly harmonic; it, therefore, is better suited to the problem of minimizing the harmonic energy.

The preconditioned conjugate gradients (PCG) algorithm allows us to take advantage of both the properties of the hat functions and those of PL harmonic wavelets. We compute $E[f]$ using the basis of hat functions, but we compute its gradient with respect to the basis of PL harmonic wavelets.

In more detail, recall that

$$g = \sum_v c^v \hat{\phi}_v = \sum d^v \psi_{h,v}\,.$$

(Because each vertex of K appears at only one level, we can drop the superscript $-k$ in the expression $\psi_{h,v}^{-k}$.) Thus, $E = E(c) = E(d)$. By the chain rule

$$\text{grad}(E) = \sum_w \frac{\partial E}{\partial d^w}\frac{\partial}{\partial d^w} = \sum_w \sum_u \frac{\partial c^u}{\partial d^w}\frac{\partial E}{\partial c^u}\frac{\partial}{\partial d^w} = \sum_v \sum_u \sum_w \frac{\partial c^u}{\partial d^w}\frac{\partial E}{\partial c^u}\frac{\partial c^v}{\partial d^w}\frac{\partial}{\partial c^v}\,.$$

Recall that $c^u = S_w^u d^w$, where S_v^u is the matrix defining the synthesis operation. Thus, the gradient can we written in the form

$$\text{grad}(E) = \sum_v \sum_u \frac{\partial E}{\partial c^u} B^{u,v} \frac{\partial}{\partial c^v}\,, \text{ where } B^{u,v} = \sum_w \frac{\partial c^u}{\partial d^w}\frac{\partial c^v}{\partial d^w} = \sum_w S_w^u S_w^v\,. \tag{6.1}$$

The matrix $B = (B^{u,v}) = S \cdot S^T$ is the "preconditioner" for our conjugate gradients algorithm. An algorithm similar to the one for computing S can be used to rapidly compute B in $O(n)$ computations (where n is the number of vertices of K). Thus, each iteration of PCG can, therefore, be done in $O(n)$ time.

6.1. **Description of Multigrid algorithm.** We also experimented with two simple multigrid approaches to finding PL harmonic maps, which we call *multigrid conjugate gradients* (MCG) and *multigrid preconditioned conjugate gradients* (MPCG). Recall that our mesh reduction algorithm furnishes us with a hierarchy of increasingly complex meshes (K_{-k}, f_{-k}), $k = J, \ldots, 1, 0$, approximating the original mesh (K, M). In this approach either CG or PCG is used to find a harmonic map on a coarse level mesh. We then use our interpolation operation to extend the map to a finer level and use that extension as the initial guess for CG or PCG at the finer level. We repeat this process until the finest level is reached.

6.2. **Numerical experiments.** To compare the performance of CG, PCG, MCG, and MPCG, we experimented with two sequences of increasingly large geodesic disks taken from the a mesh representing a small plastic bunny[3]. Our numerical experiments, which cover a range of 4 orders of magnitude, indicate that both PCG and MPCG have order of growth $O(n \log n)$ in the number of vertices. MCG and CG appear to have $O(n^2)$ order of growth.

To obtain a machine-independent measure of computation cost, we defined a "cost function" Cost(n). For each of the two algorithms, CG and PCG, we let

$$\text{Cost}(n) = \text{its} * n\,,$$

where n is the number of vertices of K and its is the number of iterations performed to achieve convergence to within a fixed tolerance. To measure the cost of the multigrid algorithms $MPCG$ and MCG, recall that a harmonic embedding is found for each of the meshes K_0, K_{-2}, K_{-4}, ... , If the number of vertices in K_{-2k} is n_k, then the cost of preconditioned conjugate gradients (PCG)is proportional to the product $\text{its}_k n_k$, where its_k is the

[3]The bunny mesh was supplied to us by Marc Levoy and his students at Stanford University

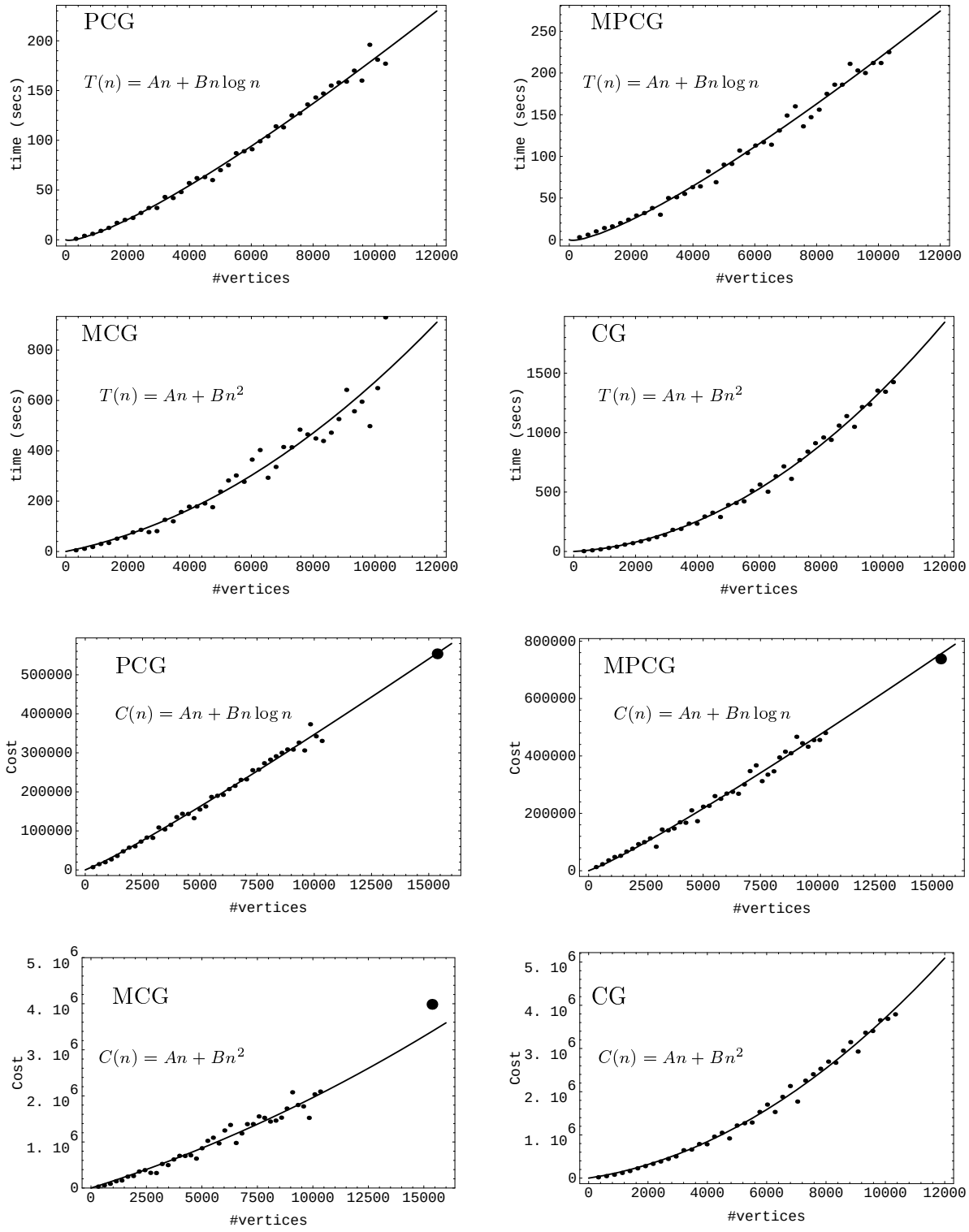

FIGURE 9. Least squares fits to the observed computational time and cost for a sequence of 40 disks ranging in size from 319 to 10329 vertices (small dots). The large dot is the computational cost of computing the harmonic map of a larger disk of 15369 vertices. The sequence of disks was taken from the "bunny mesh."

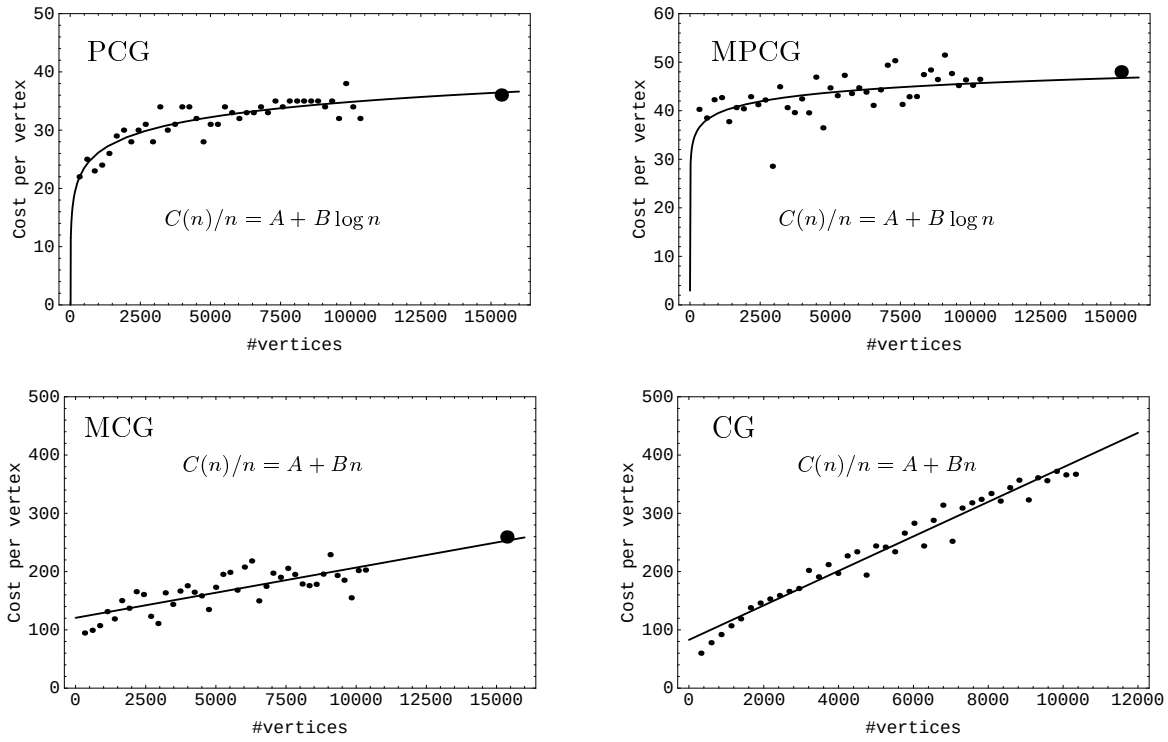

FIGURE 10. Least squares fits to the observed computational cost per vertex for a sequence of 40 disks ranging in size from 319 to 10329 vertices (small dots). The large dot is the computational cost of computing the harmonic map of a larger disk of 15369 vertices. The sequence of disks was taken from the "bunny mesh".

number of iterations of PCG required to compute the harmonic embedding of K_{2k}. Thus, the computational cost $\mathrm{Cost}(n)$ of our multigrid algorithm is proportional to the sum

$$\mathrm{Cost}(n) = \sum_k \mathrm{its}_k * n_k \,.$$

Figures 9 and 10 summarize our numerical experiments.[4]

[4]Computations were done on a DEC Alpha 500/266, equipped with 126MB of physical memory, rated at 1200MIPS peak.

References

[1] Lipman Bers. *Riemann surfaces*. Courant Institute of Mathematical Sciences, New York University, New York, 1958.

[2] Andrew Certain, Jovan Popović, Tony DeRose, Tom Duchamp, David Salesin, and Werner Stuetzle. Interactive multiresolution surface viewing. In *SIGGRAPH'96*, Computer Graphics Annual Conference Series, pages 91–98, August 1996.

[3] Gustave Choquet. Sur un type de transformation analytique généaralisant la représentation conforme et définie au moyen de functions harmoniques. *C.R.Acad. Sci.Paris, Serie 2*, 69, 1945.

[4] Matthias Eck, Tony DeRose, Tom Duchamp, Hugues Hoppe, Michael Lounsbery, and Werner Stuetzle. Multiresolution analysis of arbitrary meshes. In *SIGGRAPH'95*, Computer Graphics Annual Conference Series, pages 173–182, August 1995.

[5] G. H. Golub and C. F. Van Loan. *Matrix Computations*. Johns Hopkins University Press, Baltimore, 1989.

[6] C. M. Grimm and J. F. Hugues. Modeling surfaces of arbitrary topology using manifolds. In *SIGGRAPH'95*, Computer Graphics Annual Conference Series, pages 359–368, August 1995.

[7] David Kirkpatrick. Optimal search in planar subdivisions. *SIAM J. Computation*, 12:28–35, 1983.

[8] H. Kneser. Lösung 41. *Jahresbericht der Deutschen Math.-Vereinigung*, 35, 1927.

[9] A. Lee. Personal communication, 1997.

[10] M. J. Lounsbery. *Multiresolution Analysis for Surfaces of Arbitrary Topological Type*. PhD thesis, University of Washington, Department of Computer Science and Engineering, September 1994.

[11] M. J. Lounsbery, T. DeRose, and J. Warren. Multiresolution surfaces of arbitrary topological type. *ACM Transactions on Graphics*, 16(3):34–73, 1997.

[12] P. Schröder and W. Sweldens. Personal communication, Dec 1995.

[13] P. Schröder and W. Sweldens. Spherical wavelets: Efficiently representing functions on the sphere. In *SIGGRAPH'95*, Computer Graphics Annual Conference Series, pages 161–172, Aug 1995.

[14] William J. Schroeder, Jonathan A. Zarge, and William E. Lorensen. Decimation of triangle meshes. In *SIGGRAPH '92*, Computer Graphics Annual Conference Series, pages 65–70, 1992.

[15] W. Sweldens. The lifting scheme: A construction of second generation wavelets. *SIAM J. Math. Anal.*, 29(2):511–546, 1997.

T. Duchamp, Manifold Graphics, Inc. and Dept. of Mathematics, University of Washington

A. Certain, Manifold Graphics, Inc.

A. DeRose, Pixar, Inc. and Manifold Graphics, Inc.

W. Stuetzle, Manifold Graphics, Inc. and Dept. of Statistics, University of Washington